IEEE/CSC & ESAS SUPERCONDUCTIVITY NEWS FORUM (global edition), January 2017 (Preview 2).
This ASC 2016 manuscript 1LOr3B-06 was submitted to *IEEE Trans. Appl. Supercond.* for possible publication.
DOI: 10.1109/TASC.2016.2631938

Impact of remanent magnetic field on the heat load of original CEBAF cryomodule

Gianluigi Ciovati, Guangfeng Cheng, Michael Drury, John Fischer, and Rongli Geng

***Abstract*—The heat load of the original cryomodules for the CEBAF accelerator is ~50% higher than the target value of 100 W at 2.07 K for refurbished cavities operating at an accelerating gradient of 12.5 MV/m. This issue is due to the quality factor of the cavities being ~50% lower in the cryomodule than when tested in a vertical cryostat, even at low RF field. Previous studies were not conclusive about the origin of the additional losses. We present the results of a systematic study of the additional losses in a five-cell cavity from a de-commissioned cryomodule after attaching components, which are part of the cryomodule, such as the cold tuner, the He tank and the cold magnetic shield, prior to cryogenic testing in a vertical cryostat. Flux-gate magnetometers and temperature sensors are used as diagnostic elements. Different cool-down procedures and tests in different residual magnetic fields were investigated during the study. Three flux-gate magnetometers attached to one of the cavities installed in the refurbished cryomodule C50-12 confirmed the hypothesis of high residual magnetic field as a major cause for the increased RF losses.**

***Index Terms*—superconducting resonators, magnetic remanence, cryomodules, niobium.**

I. Introduction

THE CONTINUOUS Electron Beam Accelerator Facility (CEBAF) is a superconducting radio-frequency (SRF) accelerator which was installed at Jefferson Lab in 1994 [1]. It consists of two continuous-wave linear accelerators in a race-track design and it has been recently upgraded to deliver an electron beam with energy of 12 GeV [2]. Acceleration is provided by 418 SRF cavities resonating at 1.497 GHz, distributed in 50 cryomodules plus two cryomodules and a quarter-cryomodule in the injector. Each of the original 40 cryomodules consists of four cryounits joined inside a common vacuum vessel. Each cryounit has two SRF cavities inside a 61 cm diameter He vessel. A schematic of the cryounit is shown in Fig. 1 [3].

The original 20 cryomodules (labelled "C20") were designed to provide an energy gain of 20 MeV with a dynamic heat load of ~45 W at 2.07 K. Such specifications were exceeded during the construction of the accelerator, however it was noticed that the quality factor of the cavities, Q_0, degraded from an average of ~1×10^{10} when the cavities were tested as isolated pairs inside a vertical cryostat to an average of ~5×10^{9} when the cavities were tested inside the cryomodules, with all ancillary components, such as tuners, He vessel and fundamental power coupler (FPC) waveguide, assembled [4]. Since 2007, twelve cryomodules with the lowest performing cavities have been refurbished to allow re-processing of the cavities with better treatments (most notably high-pressure water rinsing, hydrogen degassing and electropolishing) in order to achieve a higher accelerating gradient, E_{acc} = 12.5 MV/m, resulting in an energy gain per cryomodule of 50 MeV (the refurbished cryomodules were re-labelled "C50"). In addition, a Nb "dog-leg" waveguide was added between the cavity FPC waveguide and the cold window to mitigate arcing. No other design changes were made to the cryomodule components during the refurbishment. Given the fixed cooling power of the cryoplant, the specification for the quality factor of the C50 cavities was raised to 8×10^{9} to keep the dynamic heat load of the C50 cryomodules to ~80 W. Whereas both E_{acc} and Q_0 specifications were met during the vertical test of C50 cavity pairs, the average quality factor was still ~5×10^{9} when tested in the full cryomodule, already at low field [5].

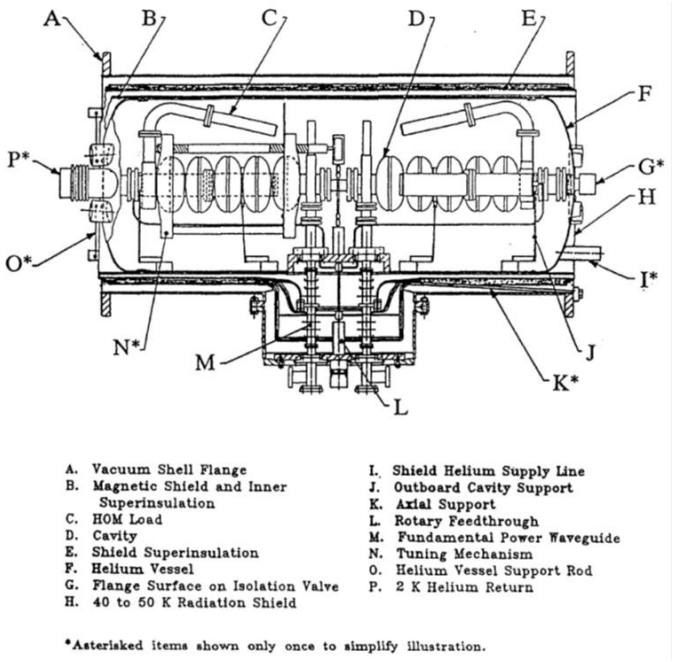

Fig. 1. Schematic of the cryounit of an original CEBAF cryomodule. It has two 5-cell cavities with tuners, inside a common He vessel [3]. A high permeability sheet wrapped around the He vessel is the inner magnetic shield and a second sheet, just inside the vacuum vessel, provides the outer magnetic shield (not shown in the figure).

This work was supported by Jefferson Science Associates, LLC, by means of Contract DE-AC05-06OR23177 from the U.S. Department of Energy.

The authors are with Jefferson Lab, Newport News, VA 23606 USA (e-mail: gciovati@jlab.org.).

Between 2010 and 2014, ten new cryomodules (labelled "C100") were built to provide an average energy gain of 100 MeV. The design of both cavities and cryomodules was significantly different than the original one and the performance specifications ($Q_0 = 8\times10^9$ at $E_{acc} = 19.7$ MV/m) were met both in the vertical tests and in the full cryomodules [6].

Initial investigations of the Q_0-degradation in the original cryomodules showed that, in some case, the degradation was related to "Q-disease" [7] and heating of the cold FPC window [4]. However, "Q-disease" could not be a prevalent cause for the Q_0-degradation because C50 cavities have been hydrogen degassed. Further investigations focused on the possibility of high residual magnetic field, a well-known cause of increased surface resistance in Nb cavities [7]. High remanent magnetic field was found in the tuner ball screw and a mu-metal box was installed around it starting with the assembly of C50-6 onward [8]. Additional tuner components (strut springs, tuner rod and bearings) with high remanent fields were later discovered and replaced with non-magnetic ones in C50-11 [9]. In spite of these efforts the average low-field Q_0 of the cavities in the cryomodules remained ~5×10^9.

In the following sections we describe the results from systematic measurements of Q_0 of a C20 cavity in a vertical cryostat, after assembling different cryomodule components, and of the residual magnetic field at the equator of a C50 cavity throughout the assembly of the latest C50 cryomodule (C50-12).

II. Results from Vertical Tests

The C20 cavity IA366 was disassembled from the cryomodule FEL02, which was going to be refurbished into cryomodule C50-12. The low-field Q_0 of the cavity in the cryomodule was 5×10^9 at 2.07 K and 5 MV/m. After disassembly, the cavity was just degreased and high-pressure rinsed then assembled with input and pick-up beam-line antennae, evacuated, isolated and attached to a vertical test stand. All other ports were blanked with Nb plates. Three single-axis flux-gate magnetometers (Mag-F, Bartington Instruments, Ltd.) were attached with Kapton tape to the top, middle and bottom cells to measure the residual field, B_{res}, close to the cavity. The sensors at the top and bottom cells are located along the side-wall, at ~45° from the vertical cavity axis, whereas the middle sensor is tangential to the equator. Three calibrated Cernox resistor-temperature devices were also attached within ~2 cm from the location of the magnetometers to measure the local temperature of the cavity. The test stand with the cavity was inserted in dewar 3 of Jefferson Lab's Vertical Test Area (VTA) and cooled from the bottom with liquid He to 4.3 K. Pumping on the He bath allowed lowering the temperature to 1.6 K. $Q_0(T)$ at a peak surface magnetic field, B_p, of 8 mT (B_p/E_{acc} = 4.56 mT/(MV/m) for the C20/C50 cavity shape) was measured between 4.3 K and 1.6 K and at different RF field levels, up to ~20 mT in the temperature range 1.6–2.0 K. $Q_0(E_{acc})$ was measured at 2.07 K for all the passband modes of the TM_{010} family. A similar protocol was followed in all subsequent RF tests. A summary of all the RF test results along with cool-down rates and residual magnetic field at 10 K is given in Table I, whereas a summary of all the $Q_0(E_{acc})$ data at 2.0 K is shown in Fig. 2. The temperature gradient dT/dz between the top and bottom cells when the temperature of the bottom cell reached the critical temperature of niobium (T_c = 9.25 K) is also listed in Table I for all tests. In all cases, the cavity was limited by a quench at ~15 MV/m, without field emission.

After this baseline test (test 1), the same tuner, which was assembled onto the cavity inside the cryomodule, was attached to the cavity and the top and bottom magnetometers were attached on the cells' side wall at 70° and 60° from the vertical axis, respectively. Fig. 3(a) shows a picture of the cavity with the tuner assembled. The cavity was then cooled to 4.3 K in dewar 3 and another RF test (test 2) was performed. The low-field Q_0 was ~15% lower than in the baseline test. Afterwards, the cavity was warmed to 30 K and cooled back down to 4.3 K with a faster cooling rate dT/dt as the local temperature crossed T_c. Another RF test was performed (test 3) but there was no significant change in Q_0. The next two tests were done after changing the residual magnetic field in the dewar to 50–100 mG over the cavity length, test 4 was done with a slow cool-down through T_c whereas test 5 was done after warming-up to 20 K and subsequent fast cool-down through T_c. In both cases, the Q_0 was ~50% lower than in the baseline test and the value at 2.07 K was measured to be 6×10^9 at 5 MV/m, comparable to what is measured on cavities inside cryomodules. The following RF test (no. 6) was done after warming the cavity to ~90 K and maintaining it in the range 90-110 K for ~26 h. The residual magnetic field in the dewar was re-adjusted to 10 mG and the cavity was cooled back down to 4.3 K. The Q_0(2.0 K, 2 MV/m) was 8×10^8 because of the "Q-disease" due to high interstitial hydrogen in the Nb.

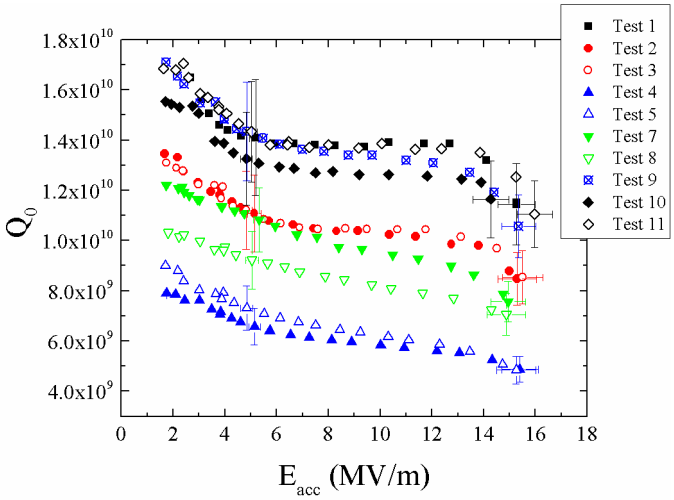

Fig. 2. Summary of $Q_0(E_{acc})$ curves for cavity IA366 measured at 2.0 K in a vertical cryostat.

After this series of tests, the cavity with tuner, under static vacuum, was moved to a different test stand and the high-permeability sheet, 0.36 mm thick (Co-NETIC AA Perfection Annealed foil, Magnetic Shield Corp.) used to provide the inner magnetic shielding in the cryounit was wrapped around

IEEE/CSC & ESAS SUPERCONDUCTIVITY NEWS FORUM (global edition), January 2017 (Preview 2).
This ASC 2016 manuscript 1LOr3B-06 was submitted to *IEEE Trans. Appl. Supercond.* for possible publication.
DOI: 10.1109/TASC.2016.2631938

the cavity. The magnetometers at top and bottom were attached to the aluminum tuner frames clamped to the end cells and oriented to measure the vertical field component. The magnetometer at the equator of the middle-cell was also oriented to measure the vertical field component. The test stand was inserted into dewar 8 and the residual magnetic field was re-adjusted to an average of 50 mG over the cavity length. The cavity was cooled to 4.3 K and the RF measurements (test 7) showed a similar Q_0-value to what was measured for the cavity with the tuner only, in low residual field. The cavity was then warmed up to 300 K, the magnetic shield was removed and the cavity was cooled back down to 4.3 K in the same residual field (~50 mG) as in the previous test. The Q_0 at 5 MV/m measured in test 8 was ~18% lower than the previous test, confirming the shielding efficacy of the high-μ sheet.

In preparation for the next RF test, the tuner was removed and all the components were degaussed with a surface demagnetizer, reducing the remanent field on contact from several Gauss to ~0.1 G. The tuner strut springs were replaced with new ones made of stainless steel 316L. The tuner was re-assembled onto the cavity which was then inserted in dewar 7. The results from RF test 9 showed that the Q_0 had recovered to the value achieved during the baseline test, without tuner.

The next component, which is close to the cavity inside the cryomodule, is the He tank. A survey of the remanent field of the cylindrical stainless steel He vessels removed from FEL02 showed fields up to ~700 mG on contact at the location of the instrumentation port on the vessel and ~100 mG on contact at places where welds had been ground. Such fields result in regions with ~10 mG above background at the cavities' equator location. One of the He vessel's cylinders was tack-welded to a He vessel head, suspended around the cavity with tuner. Fig. 3(b) shows a picture of the test stand with cavity, tuner and He vessel. The test stand was inserted into dewar 5 and cooled to 4.3 K. The results from RF test 10 showed no significant change of Q_0 from the previous test. The cavity was warmed up to 16 K and slowly cooled through T_c, in preparation for RF test 11. The test results showed a marginal increase of Q_0, due to a reduction of the ambient field in the dewar.

TABLE I
SUMMARY OF VERTICAL TEST RESULTS

Test No.	dT/dt at 9 K (K/min)	dT/dz (K/cm)	B_{res} at 10 K (mG)	Q_0(2.0 K, 5 MV/m)
1	1.7 ± 0.2	2.6	2.8 ± 0.2	$(1.3 \pm 0.2)\times10^{10}$
2	1.9 ± 0.4	3.7	11 – 43	$(1.1 \pm 0.2)\times10^{10}$
3	7.4 – 14	0.1	22 – 35	$(1.1 \pm 0.2)\times10^{10}$
4	0.05 ± 0.01	0.03	27 – 137	$(6.6 \pm 0.7)\times10^{9}$
5	3.5 ± 0.1	2.4	6 – 120	$(7.3 \pm 0.9)\times10^{9}$
6	1.6 ± 0.7	1.3	20 – 45	$(8 \pm 5)\times10^{8}$
7	1.8 ± 0.7	3.8	5 – 80	$(1.1 \pm 0.1)\times10^{10}$
8	3.5 – 22	3.8	46 ± 9	$(9.2 \pm 1.2)\times10^{9}$
9	2.8 – 16	3.2	4 – 23	$(1.4 \pm 0.2)\times10^{10}$
10	0.9 ± 0.6	3.9	8 ± 2	$(1.3 \pm 0.2)\times10^{10}$
11	0.1 – 0.4	0.06	4 ± 3	$(1.4 \pm 0.2)\times10^{10}$

The values of cooling rates and residual field are given as average with standard deviation if they are uniform along the cavity, as a range of values otherwise. Only the vertical (major) component of B_{res} is listed in the table.

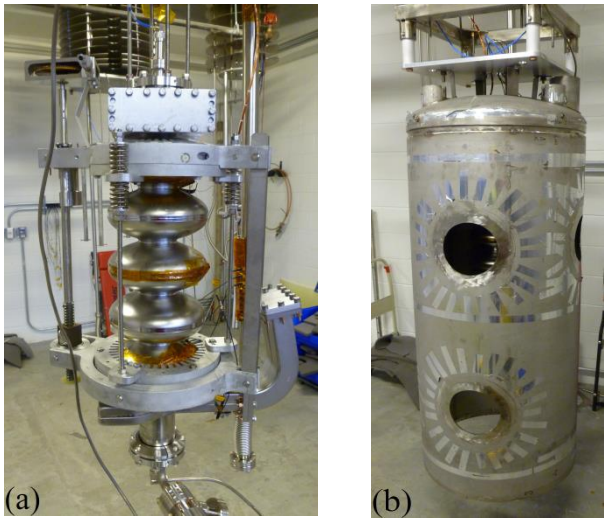

Fig. 3. Pictures of the cavity IA366 with tuner (a) and with tuner and He vessel (b) hanging from a vertical test stand.

III. RESULTS FROM CRYOMODULE ASSEMBLY AND TEST

The tuner components and He vessels for all cavities to be installed into C50-12 were degaussed with a surface demagnetizer, reducing the remanent field on contact to ~50 mG. In order to monitor the residual magnetic field at a cavity location throughout the assembly and testing of the cryomodule, three single-axis flux-gate magnetometers of the same type used for the vertical test study were attached close or onto the equator of the end-cells and middle cell of cavity IA367, as shown schematically in Fig. 4. The sensors on the end-cells, at both FPC and high-order-mode (HOM) sides, measure the axial magnetic field component, whereas the sensor on the middle cell measure the azimuthal component. No sensor was placed in the transverse direction as that was considered to be the field orientation to be best attenuated by the cylindrical magnetic shield. Temperature diodes were also attached to the bottom of the tuner brackets on the equators of the end cells and at the top of the equator of the middle cell.

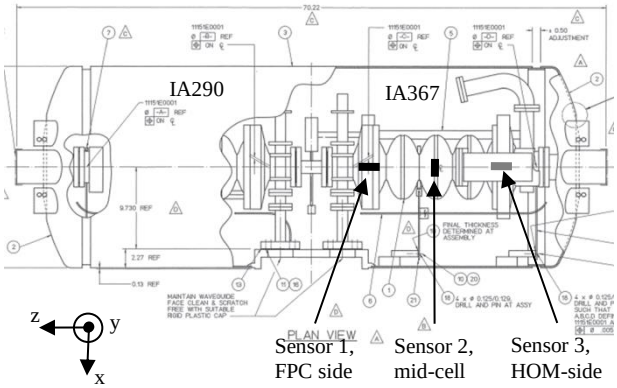

Fig. 4. Schematic of the top view of the cryunit with cavities IA367 and IA290, showing the location of the three single-axis flux-gate magnetometers.

Fig. 5 shows a summary of the residual fields measured on cavity IA367 through cryomodule assembly, in the Test Cave and after testing. The background field in the assembly area and the high-bay location where the cryomodule was moved to

IEEE/CSC & ESAS SUPERCONDUCTIVITY NEWS FORUM (global edition), January 2017 (Preview 2).
This ASC 2016 manuscript 1LOr3B-06 was submitted to *IEEE Trans. Appl. Supercond.* for possible publication.
DOI: 10.1109/TASC.2016.2631938

after testing was ~0.5 G, whereas it is a factor of ten lower in the Cryomodule Test Facility (CMTF) and ~0.7 G in the CEBAF tunnel. Further details about the residual field measurements are given in [10].

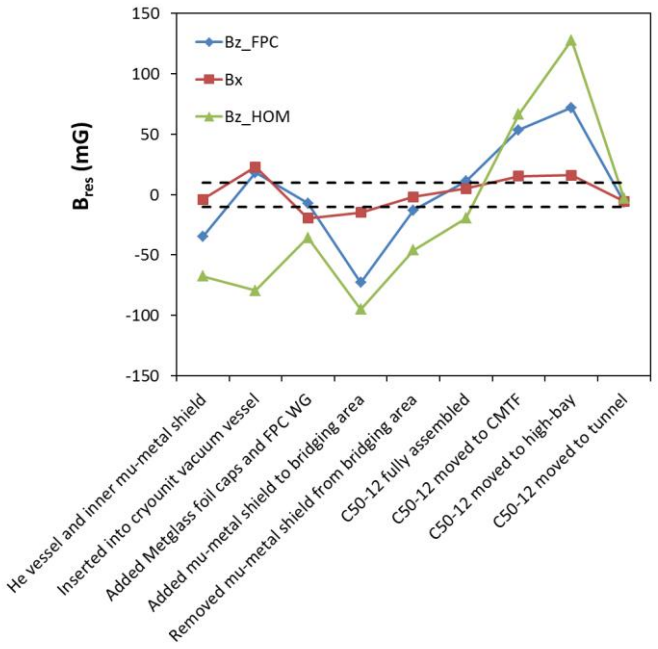

Fig. 5. Residual magnetic field measured at room temperature at the equators of cavity IA367 during assembly, prior to and after testing in cryomodule C50-12. The dashed lines represent the specifications being ±10 mG.

A check of the residual field on one cavity pair, before assembly into the He vessel revealed that the assembly rails had high remanent field decaying to ~100 mG at the equator locations and that some of the tuner strut-springs added an additional ~20-40 mG to the residual field at the equator locations. It was also found that:

- the gate valves at both ends of the cavity pair were not degaussed and had a remanent field on contact of 1.5-2.5 G.
- welding of the He supply and return piping between cryounit created regions with remanent field on contact of 1-1.5 G
- both gate valves and He piping are in the bridging area between cryounits and the addition of the magnetic shield in this area focuses the residual field towards the inner volume of the cryomodule. Therefore it was decided to remove shielding from this area. Fig. 6 shows a picture of the assembled cryounit and of the bridging area.

Both ends of the He vessels were covered with 20 layers of a high-permeability alloy foil (2605SA1, Metglass, Inc.) to help reducing the axial field leaking into the He vessel.

Fig. 7 shows a summary of the low-field Q_0-values measured in seven of the eight cavities in C50-12 when tested as cavity pairs in the VTA and inside the cryomodule in the CMTF and in the CEBAF tunnel. One of the cavities was not tested due to issues with waveguide vacuum. The results from the test in the CMTF showed that only two of the cavities (IA027 and IA029) had a Q_0-value within experimental uncertainty from what was measured in the vertical test. The Q_0-value of IA367 in the cryomodule test in the CMTF was about a factor of two lower than in the vertical test and it is consistent with the magnitude of the residual field measured at the equator. The amplitude of the axial field was reduced by ~20% from 300 K to 4.3 K. However, Q_0 was higher when the cryomodule was tested in the CEBAF tunnel, as shown in Fig. 7, consistent with the lower residual magnetic field measured at cavity IA367.

Fig. 6. Picture of the fully assembled cryounit with cavity IA367. The bridging area to the next cryounit is visible on the right side.

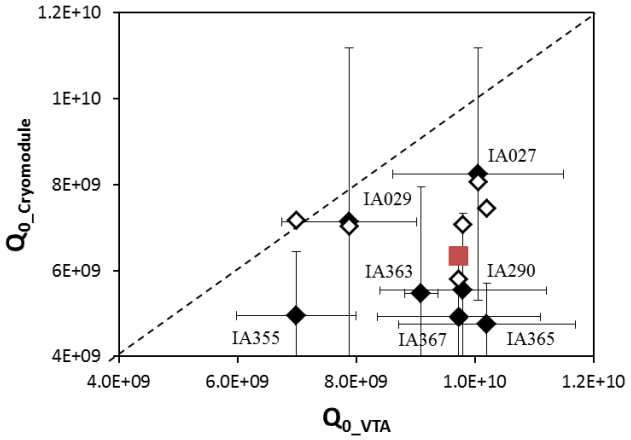

Fig. 7. Q_0-values measured in the vertical cryostat and in the cryomodule at 2.07 K and 5 MV/m for cavities installed in C50-12. The solid symbols refer to measurements in the CMTF, whereas empty symbols refer to measurements in the tunnel. The red square is the estimated Q_0-value for cavity IA367 based on the average B_{res} at the cavity in the CMTF. The measurement of the Q_0 of cavity IA363 in the tunnel is not yet completed. The dashed line is a guide to the eye representing equal Q_0-values in the VTA and CMTF.

IV. Data Analysis and Discussion

From the measurements of the low-field Q_0 of the TM_{010} passband, it is possible to obtain information about the surface resistance of individual cavity cells. Because of the symmetry of the field distribution with respect to the cavity center in the TM_{010} passband, differences in R_s between cells 1 and 5 and between cells 2 and 4 cannot be distinguished. The surface resistance of cells 1 and 5, $R_{s1,5}$, that of cells 2 and 4, $R_{s2,4}$, and that of cell 3, R_{s3}, can be calculated by solving the following system of three equations in three unknowns:

$$2R_{s1,5}\int_A \left(H_{i,1,5}/H_{p,i}\right)^2 da + 2R_{s2,4}\int_A \left(H_{i,2,4}/H_{p,i}\right)^2 da + R_{s3}\int_A \left(H_{i,3}/H_{p,i}\right)^2 da = \frac{4\pi f_i}{Q_{0,i}\alpha_i} \quad i = 0,1,2 \tag{1}$$

where i is the mode index, for any three of the five passband modes, f_i is the resonant frequency of mode i, $\alpha_i = H^2_{p,i}/U_i$ is a coefficient calculated for each mode with SUPERFISH, a finite difference electromagnetic code [11] (U_i is the stored energy for mode i) and the integrals are over the area of a cell, A, and they are also calculated from SUPERFISH for each mode. The results showed that the middle cell has the lowest R_s (~14 nΩ, compared to ~25 nΩ for the other cells) and that after tuner assembly (Test 2) the end cells had the largest increase in R_s (~7–9 nΩ), consistent with the remanent field of the strut spring located close to those cells.

The average cavity surface resistance, R_s, of the TM_{010}-π mode can be obtained from the measured Q_0-values as $R_s = G/Q_0$, where G = 274 Ω is a geometry factor calculated with SUPERFISH. The temperature dependence of R_s is described as:

$$R_s(T) = R_{BCS}(T, \Delta/k_B T_c, \ell) + R_{res} \tag{2}$$

where R_{BCS} is the Bardeen-Cooper-Schrieffer surface resistance calculated with a numerical code [12], R_{res} is the residual resistance, Δ is the energy gap at 0 K, k_B is Boltzmann's constant and ℓ is the mean free path. $R_s(T)$ data were measured at different fields, in the 8-20 mT range and fit of the data with Eq. (2) showed that R_{res} increases linearly with increasing B_p within this range, as shown for example in Fig. 8 for Test 1. This dependence had been previously found in cavities with a high concentration of interstitial hydrogen [13].

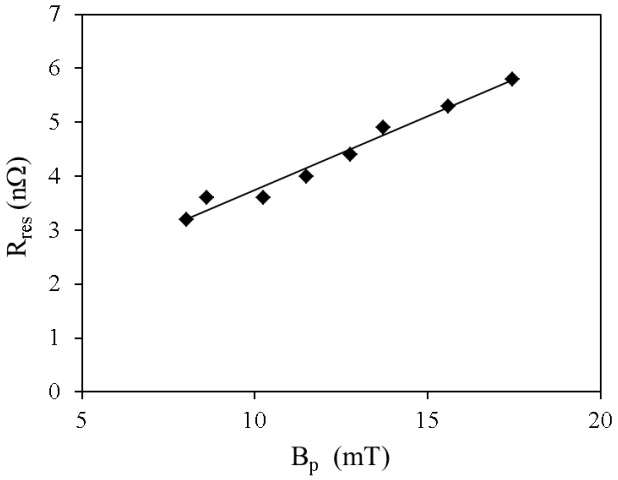

Fig. 8. R_{res} as a function of the peak surface rf magnetic field obtained from Test 1. The solid line is a linear fit to the data.

$R_{res}(B_p)$ was then described as:

$$R_{res}(B_p) = dR_{res}/dB_p\, B_p + R_{res0}. \tag{3}$$

The values of the zero-field intercept R_{res0} and of the slope dR_{res}/dB_p plotted as a function of the average B_{res} over the cavity length, for the different tests, are shown in Fig. 9. R_{res0} increases approximately linearly with B_{res} at a rate of 0.2 nΩ/mG, consistent with results from earlier studies on the impact of residual magnetic field on the residual resistance [14–17]. dR_{res}/dB_p also seems to increase linearly with B_{res} at a rate of 2.9 (nΩ/T)/mG.

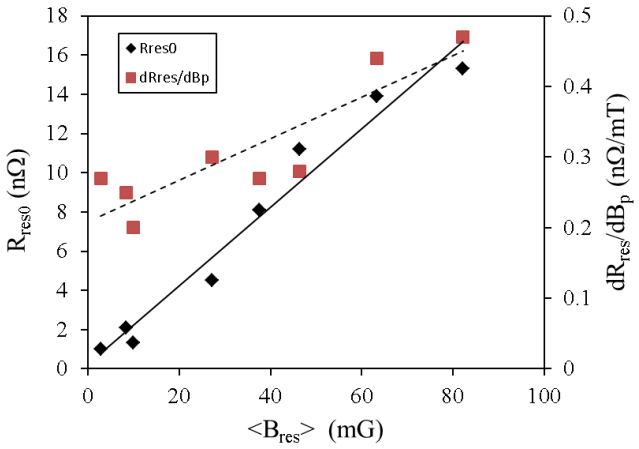

Fig. 9. R_{res0} and dR_{res}/dB_p as a function of the average residual field. Lines are linear fit to the data.

Recent studies of flux expulsion in bulk Nb cavities showed that higher Q_0, related to increased flux expulsion, could be achieved in the presence of temperature gradients of ~0.1 K/cm at T_c [18–22]. However, it was also found that the flux expulsion efficiency strongly depends on the grain size and treatment [17, 21, 22]. The results on cavity IA366 showed no significant change of Q_0 with different cooling rates or temperature gradients, as shown in Table I. The ratio of B_{res} below and above T_c measured at the top and bottom equators was in the range 0.8 – 1.1, regardless of the temperature gradient at T_c. The poor flux expulsion of IA366 could be due to the presence of sub-micron size hydrides because of the high concentration of interstitial hydrogen. Cavity IA367, which had been degassed at 600 °C for 10 h, also had negligible flux expulsion during the cooldown in the CMTF, as shown in Fig. 10. The whole cavity was at a uniform temperature (longitudinal and transverse gradients less than 0.02 K/cm) while cooling below T_c at a rate of ~3 K/min. Cavities IA080 and IA355 had been annealed at ~1400 °C in the past, which resulted in Nb grains of ~1 mm size, the Q_0-value of IA355 was not significantly different than that of IA367 when tested in the CMTF, as shown in Fig. 7.

Remarkably, it was found that the residual field measured at a cavity equators changes significantly depending on the cryomodule location, with the lowest fields being measured when the cyromodule was installed in the CEBAF tunnel. This

might be explained as being due to the residual ambient field leaking inside the cryomodule and either adding or subtracting to the remanent field of magnetized components, depending on the orientation of the cryomodule with respect to the ambient field.

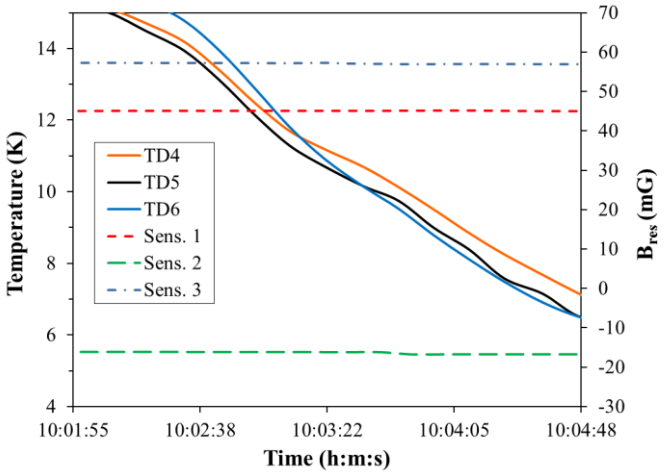

Fig. 10. Temperature and residual field at cavity IA367 during cooldown of C50-12 below 9.25 K in the CMTF. TD4 is located at the bottom of the equator of the end cell on the FPC side, TD5 is located on top of the equator of the center cell and TD6 is located at the bottom of the equator of the other end-cell.

V. Conclusion

A systematic study of the impact of magnetized components on the quality factor of 5-cell cavities used in the CEBAF accelerator showed a degradation of Q_0 by ~15% when tested in a vertical cryostat. An effort was made to degauss the components closest to the cavity during the refurbishment of the cryomodule C50-12.

The results from the cryomodule test in the CMTF showed that the Q_0 was still low, about 5×10^9 at 2.07 K, 5 MV/m, in five cavities. The residual field of ~50 mG measured at a cavity location inside the cryomodule can explain ~75% of the Q_0-degradation. Considering that the amplitude of the residual magnetic field was not measured in the transverse direction, even better agreement between the magnitude of B_{res} and the Q_0-degradation can be expected. Another source of additional RF losses in the cavity inside the cryomodule can be the metallization used for brazing of the cold FPC window. When testing a cavity in the cryomodule, ~500 W of forward power are needed to reach a gradient of 5 MV/m, compared to ~2 W during the vertical test, because of the different coupling. The contribution of window losses to the RF heat load is being investigated both experimentally and through computer-aided RF calculations.

The results from the cryomodule test in the CEBAF tunnel showed significantly higher Q_0-values than in the CMTF, with several cavities having among the highest Q_0 measured in an original CEBAF cryomodule. A lower residual field was also measured at the equator of cavity IA367 than in the CMTF. The explanation for this could be the interaction of the ambient field leaking into the cryomodule with the remanent field of cryomodule components.

During the cryomodule assembly, it was found that the inner magnetic shield is too far from the cavity and can actually focus any remanent field inside the cryomodule. In addition, it was also found that controlling the magnetization of components with high permeability throughout the cryomodule assembly process can be a challenging task.

A possible convenient way to mitigate the issue is to attempt degaussing of an entire, fully assembled cryomodule, as it was recently shown at FNAL with the prototype cryomodule for the LCLS-II project [23]. Such degaussing has been proposed for the accelerator maintenance shutdown in 2017. In preparation for the refurbishment of the next C50 cryomodule, it is proposed to revisit the design of the magnetic shield and to improve the quality control of components with respect to remanent fields.

Acknowledgment

The authors would like to thank the Cavity Production and Cryomodule Production groups at Jefferson Lab for helping with the cavity preparation and assembly.

References

[1] H. Grunder, "CEBAF commissioning and future plans," presented at the PAC 1995 Conf., Gif sur Yvette, France, Oct. 17–20, 1995, Paper MAD01.

[2] A. Freyberger, "Commissioning and operation of 12 GeV CEBAF," presented at the IPAC 2015 Conf., Richmond, VA, USA, May 3–8, 2015, Paper MOXGB2.

[3] C. Leeman, "CEBAF design overview and project status," presented at the SRF 1987 Conf., Argonne, IL, USA, Sep. 14–18, 1987, Paper SRF87a09.

[4] W. J. Schneider, M. Drury, and J. Preble, "Anomalous Q_0 results in the CEBAF south linac," presented at the SRF 1993 Conf., Newport News, VA, USA, Oct. 4–8, 1993, Paper SRF93I13.

[5] M.A. Drury, G.K. Davis, J.F. Fischer, C. Grenoble, J. Hogan, L.K. King, K. Macha, J.D. Mammosser, C.E. Reece, A.V. Reilly, J. Saunders, H. Wang, E. Daly, J.P. Preble, "Summary report for the C50 cryomodule project," presented at the PAC 2011 Conf., New York, NY, USA, March 28–April 1, 2011, Paper TUP108.

[6] M. Drury, G. K. Davis, J. Hogan, C. Hovater, L. King, F. Marhauser, H. Park, J. Preble, C. E. Reece, R. Rimmer, H. Wang, and M. Wiseman, "CEBAF upgrade: cryomodule performance and lessons learned," presented at the SRF 2013 Conf., Paris, France, Sep. 23–27, 2013, Paper THIOB01.

[7] H. Padamsee, T. Hays, and J. Knobloch, *RF Superconductivity for Accelerators*, 1st ed. New York, USA: J. Wiley & Sons, 1998, pp. 171–177.

[8] M.A. Drury, E. Daly, G.K. Davis, J.F. Fischer, C. Grenoble, J. Hogan, F. Humphry, L.K. King, J.P. Preble, and K. Worland, "Overview of the first five refurbished CEBAF cryomodules," presented at the LINAC 2008 Conf., Victoria, BC, Canada, Sep. 29–Oct. 1, 2008, Paper THP122.

[9] R.L. Geng, J. Fischer, F.S. He, Y.M. Li, C.E. Reece, and T. Reilly, "Pursuing the origin and remediation of low Q0 observed in the original CEBAF cryomodules," presented at the IPAC 2014 Conf., Dresden, Germany, June 15–20, 2014, Paper THOBB01.

[10] G. Ciovati and G. Cheng, "Measurements of residual magnetic field on cavity IA367 in cryomodule C50-12," Jefferson Lab Technical Note 16-027, August 2016.

[11] K. Halbach and R. F. Holsinger, "SUPERFISH - A computer program for evaluation of RF cavities with cylindrical symmetry," *Part. Accel.*, vol. 7, no. 4, pp. 213–222, 1976.

[12] J. Halbritter, "FORTRAN-program for the computation of the surface impedance of superconductors", Karlsruhe Nuclear Research Center Technical Note 3/70-6, June 1970.

[13] J. Halbritter, P. Kneisel, and K. Saito, "Additional losses in high purity niobium cavities related to slow cooldown and hydrogen segregation,"

presented at the SRF 1993 Conf., Newport News, VA, USA, Oct. 4–8, 1993, Paper SRF93I08.

[14] G. Arnold-Meyer and W. Weingarten, "Comparative measurements on niobium sheet and sputter coated cavities," *IEEE Trans. Magn.,* vol. 23, no. 2, March 1987, pp. 1620–1623.

[15] P. Kneisel and B. Lewis, "Additional RF surface resistance in superconducting niobium cavities caused by trapped magnetic flux", Jefferson Lab Technical Note 94-028, 1994.

[16] C. Benvenuti, S. Calatroni, I.E. Campisi, P. Darriulat, C. Durand, M. Peck, R. Russo, and A.-M. Valente, "Magnetic flux trapping in superconducting niobium," presented at the SRF 1997 Conf., Abano Terme, Italy, Oct. 6–10, 1997, Paper TSRF97B05.

[17] G. Ciovati and A. Gurevich, "Measurement of RF losses due to trapped flux in a large-grain niobium cavity," presented at the SRF 2007 Conf., Beijing, China, Oct. 14–19, 2007, Paper TUP13.

[18] A. Romanenko, A. Grassellino, A. C. Crawford, D. A. Sergatskov, and O. Melnychuk, "Ultra-high quality factors in superconducting niobium cavities in ambient magnetic fields up to 190 mG," *Appl. Phys. Lett*., vol. 105, 2014, Art. no. 234103.

[19] D. Gonnella and M. Liepe, "Cooldown and flux trap studies on SRF cavities," presented at the LINAC 2014 Conf., Geneva, Switzerland, Aug. 31–Sep. 5, 2014, Paper MOPP017.

[20] M. Martinello, M. Checchin, A. Grassellino, A. C. Crawford, O. Melnychuk, A. Romanenko, and D. A. Sergatskov, "Magnetic flux studies in horizontally cooled elliptical superconducting cavities," *J. Appl. Phys.*, vol. 118, 2015, Art. no. 044505.

[21] S. Posen, M. Checchin, A. C. Crawford, A. Grassellino, M. Martinello, O. S. Melnychuk, A. Romanenko, D. A. Sergatskov, and Y. Trenikhina, "Efficient expulsion of magnetic flux in superconducting radiofrequency cavities for high Q_0 applications," *J. Appl. Phys.*, vol. 119, 2016, Art. no. 213903.

[22] S. Huang, T. Kubo, and R. L. Geng, "Dependence of trapped-flux-induced surface resistance of a large-grain Nb superconducting radio-frequency cavity on spatial temperature gradient during cooldown through T_c," *Phys. Rev. Accel. Beams*, vol. 19, 2016, Art. no. 082001.

[23] S. Chandrasekaran, Fermi National Accelerator Laboratory, IL, USA, private communication, 2016.